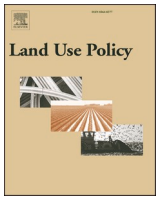
Land Use Policy 159 (2025) 107775



Contents lists available at ScienceDirect

Land Use Policy

journal homepage: www.elsevier.com/locate/landusepol





Gradual or leapfrog? Decoding the characteristics and patterns of urban redevelopment in rapidly developing megacities, China

Zhi Cai [a], He Zhu [b], Yan Tang [c,*]

[a] School of Tourism and Urban-Rural Planning, Zhejiang Gongshang University, Hangzhou 310018, PR China
[b] School of Architecture and Urban Planning, Beijing University of Civil Engineering and Architecture, Beijing 100044, PR China
[c] School of Architecture, Tsinghua University, Beijing 100084, PR China

ARTICLE INFO

Keywords:
Urban redevelopment
Urban morphology
LCZ
Patterns
Machine learning
Megacities

ABSTRACT

Traditional urban redevelopment studies have been largely confined to micro-scale analyses, leaving macro-scale, long-term dynamics poorly understood. This study addresses this gap by utilizing machine learning and multi-temporal satellite imagery, combined with an adapted Local Climate Zone (LCZ') scheme, to systematically analyze urban redevelopment patterns in three rapidly developing Chinese megacities from 1985 to 2020. Our findings reveal a three-phase evolution: Phase I (<1995), characterized by slow redevelopment that outweighed expansion; Phase II (1995–2010), marked by rapid expansion that surpassed redevelopment; and Phase III (>2010), a period of decelerated expansion where redevelopment once again became the dominant mode of urban change. This evolution has produced distinct redevelopment patterns defined by their intensity change and spatial trajectory. The primary mode is a gradual pattern, where lower-intensity built-up classes are gradually replaced by higher-intensity ones, typically expanding outward from the city center. This is contrasted with leapfrog patterns, characterized by the direct transformation of the lowest-intensity classes to the highest-intensity ones. These leapfrog dynamics manifest in two main spatial forms: a "T"-shaped leapfrog, where initial outward redevelopment is followed by a secondary wave of renewal back to the city center, and an inverse "T"-shaped leapfrog, characterized by the simultaneous inward movement of redevelopment from outer suburbs and outward movement from the inner city. While gradual redevelopment pattern were common throughout, leapfrog patterns are more commonly observed in Phase III. These findings reveal a critical shift in urban growth logic from simple expansion to complex, multi-directional redevelopment, and provide valuable empirical insights for guiding urban development and optimizing urban morphology.

1. Introduction

Urban redevelopment, a strategy for transforming urban morphology, refers to the reconstruction of built-up areas, particularly in vacant and deteriorating inner-city areas, with the aim of enhancing both the physical environment and the socio-economic conditions of the urban areas (Mele, 2013). Typically, urban redevelopment increases construction intensity on land parcels, often by transitioning from low-density to high-density development. In certain cases, however, it also engages in "demolition for green" initiatives (Kabisch and Haase, 2013; Walker et al., 2017), transforming urban built-up areas into parks and green spaces, thereby reducing construction intensity. As a pivotal component of urban development, redevelopment serves as an effective way to improve land use efficiency, curbing urban sprawl, and stimulating economic revitalization (Van Duijn et al., 2016). In essence, urban redevelopment can reshape urban structures and landscapes (Ryan, 2006), thereby contributing to the enhancement of the physical environment and influencing local microclimates (Heris et al., 2020). Consequently, the challenge of leveraging redevelopment to promote urban sustainability, while addressing intertwined economic, environmental, and climatic concerns, has emerged as a focal point of global attention in the post-urbanization era (O'Connor, 2019; Weber, 2002).

In rapidly developing cities, the transformation of urban morphology generally occurs through two primary pathways: expansion and renewal/redevelopment. Previous studies have extensively discussed the morphological changes resulting from urban expansion at the macro-scale (Alam and Banerjee, 2023; Chen et al., 2020; He et al., 2019), as these changes are more easily observable and identifiable through

* Corresponding author.
E-mail addresses: caiz19@tsinghua.org.cn (Z. Cai), zhuhe@bucea.edu.cn (H. Zhu), yantang@mail.tsinghua.edu.cn (Y. Tang).

https://doi.org/10.1016/j.landusepol.2025.107775
Received 17 April 2025; Received in revised form 1 August 2025; Accepted 22 September 2025
Available online 29 September 2025
0264-8377/© 2025 Elsevier Ltd. All rights are reserved, including those for text and data mining, AI training, and similar technologies.

map-based analyses. However, macro-scale investigations of morphological changes resulting from urban renewal/redevelopment are relatively scarce. This scarcity can be attributed, in part, to the fact that certain renewal initiatives do not directly alter urban morphology, such as urban renovation projects that preserve existing buildings and environmental layouts. Conversely, redevelopment projects that do affect urban morphology, such as the transformation of low-rise residential areas into high-rise office districts, present challenges in obtaining comprehensive data for identifying and analyzing these changes. This is because traditional methods to delineate the spatiotemporal distribution of urban redevelopment areas often rely on municipal urban planning data or field surveys (Dubé et al., 2018; Lai et al., 2021), especially at micro-scale. In recent years, advancements in technologies such as satellite remote sensing, artificial intelligence, and the opening of various big data platforms have significantly expanded the potential to identify urban redevelopment areas at macro-scale (Han et al., 2020; Ilic et al., 2019; Lin et al., 2024). For example, Ilic et al. (2019) employed deep learning techniques applied to street view images to detect building changes in gentrification areas, Lin et al.(2024) utilized machine learning methods to analyze time-series remote sensing images for urban redevelopment mapping, and Han et al. (2020) identified urban redevelopment areas using open street network and point-of-interest (POI) data. Additionally, some researchers have leveraged urban landscape features and morphological characteristics to detect redevelopment areas (Cai et al., 2022; Wen et al., 2019; Zhou et al., 2024). For instance, Wen et al. (2019) monitored urban redevelopment patterns from perspectives such as urban morphology (e.g., building density, floor area ratio) and urban functional zones (e.g., residential, commercial, and industrial).

Leveraging advanced methodologies, scholars have gained broader research perspective for delineate the spatial distribution characteristics of urban redevelopment. Most studies indicate that redevelopment is more prevalent in central urban areas (Frantál et al., 2015; Han et al., 2020; Lai et al., 2021a), while others highlight higher redevelopment potential in suburban areas (Han et al., 2022; Lai et al., 2021a). Beyond spatial identification, numerous studies have also explored the driving forces behind urban redevelopment and assessed its impacts. Previous research has found that urban redevelopment is influenced by multiple factors, including economic, political, geographical location, and stakeholders (e.g., original property owners, government agencies, and developers) (Chen et al., 2022; Li et al., 2014; Wong et al., 2021; Zhu et al., 2024). Other studies indicated that redevelopment can have substantial effects on various aspects of the urban environment, including social, economic, and environmental factors (Hong and Hong, 2016; Liu et al., 2018). For example, it can lead to neighborhood gentrification and displace original residents, thereby exacerbating social inequality (Liu et al., 2018).

While previous studies on urban redevelopment has deepened, limitations in research methodologies and perspectives persist. Despite the existence of various quantitative methods for urban analysis, integrated approaches capable of both quantitatively capturing and systematically describing the complex changes in urban morphology before and after redevelopment, particularly at the macro-scale, are still not sufficiently developed. Moreover, relatively few studies focus on analyzing the spatiotemporal evolution patterns of redevelopment activities at the city level or macro-scale. Additionally, it remains unclear whether different cities follow similar redevelopment patterns.

Consequently, it is necessary to employ a new analytical framework and empirical evidence to systematically capture urban redevelopment dynamics across multiple cities, enabling the generalization of their spatiotemporal evolution patterns at the macro-level. To address these research gaps, we comprehensively utilize emerging analytical tools and multiple data sources enabled by new information technologies, such as machine learning and satellite remote sensing to overcome the challenges inherent in large-scale, long-term, and multi-city comparative studies. We employ the Local Climate Zone (LCZ) scheme for urban morphology classification (Stewart and Oke, 2012), which categorizes urban built-up areas into ten classes, each with specific canopy parameters, such as aspect ratio, building density and height (Appendix Table 1). Compared to traditional two-dimensional land use/cover approaches, LCZ comprehensively captures the fine-grained, three-dimensional urban morphological characteristics, making it an ideal framework for identifying urban redevelopment areas and quantifying their morphological changes.

Since 1990, China has undergone rapid urbanization, with its built-up areas expanding nearly tenfold, leading to dramatic transformation of urban morphology and redevelopment characteristics. According to the China national seventh population census (State Council, 2021), by the end of 2020, China had seven megacities with populations exceeding 10 million. The permanent population residing in these megacities reached 139 million, accounting for approximately 9.85 % of the national population. It is foreseeable that, before Chinese urbanization rate stabilizes near 80 %, more cities will join the ranks of megacities in the future. Given the high concentration of both population and resources, megacities face increasing pressure in areas such as ecological environment quality and sustainable development. Moreover, challenges related to spatial disorganization and disorder are particularly prominent. In contrast, China's urban planning system has long relied on intensity indicators (e.g. floor area ratio) to control land development, lacking detailed three-dimensional guidelines (e.g. building height and urban fabric), which exacerbates issues related to the management of urban landscapes and contributes to the emergence of various urban problems. To better understand the root causes of these challenges, we select three representative megacities in China: Beijing, Shanghai, and Guangzhou, as case studies, which aims to answer the following research questions:

1) What are the characteristics of urban redevelopment in rapidly developing megacities?
2) What are the spatiotemporal evolution patterns of urban redevelopment?

Through this, we seek to deepen our understanding of urban spatial development, thereby providing empirical reference for the urban sustainable development.

2. Data and methods

2.1. Study area

As urban boundaries are continuously shifting and the sizes of built-up areas differ across cities, making comparisons between them presents certain challenges. Existing studies indicate that the effective radius of most cities in China typically falls within 36 km (Jiao, 2015; Cai et al., 2022). To standardize comparisons and capture urban boundaries comprehensively, our study area is defined as a circular region with a 36 km radius, centered on the city center (Fig. 1). Given that the city center may shift over time due to urban development or that adjacent cities may evolve into a metropolitan area with multiple cores, we use the city center of the pre-1990 urban area as the origin to mitigate such disruptions. Here, 'city center' specifically refers to a historic commercial hub or a prominent landmark square in old urban areas.

2.2. Data sources and preprocessing

This study primarily utilizes multi-temporal remote sensing imagery from the Keyhole, Landsat and Sentinel satellite series, supplemented by Google Earth's super-high-resolution historical imagery (Table 1). While Google historical imagery was sourced from Google Earth, all other satellite imagery were obtained from the U.S. Geological Survey (https://earthexplorer.usgs.gov). Given that China's rapid urbanization began in earnest after 1980, the earliest available high-resolution

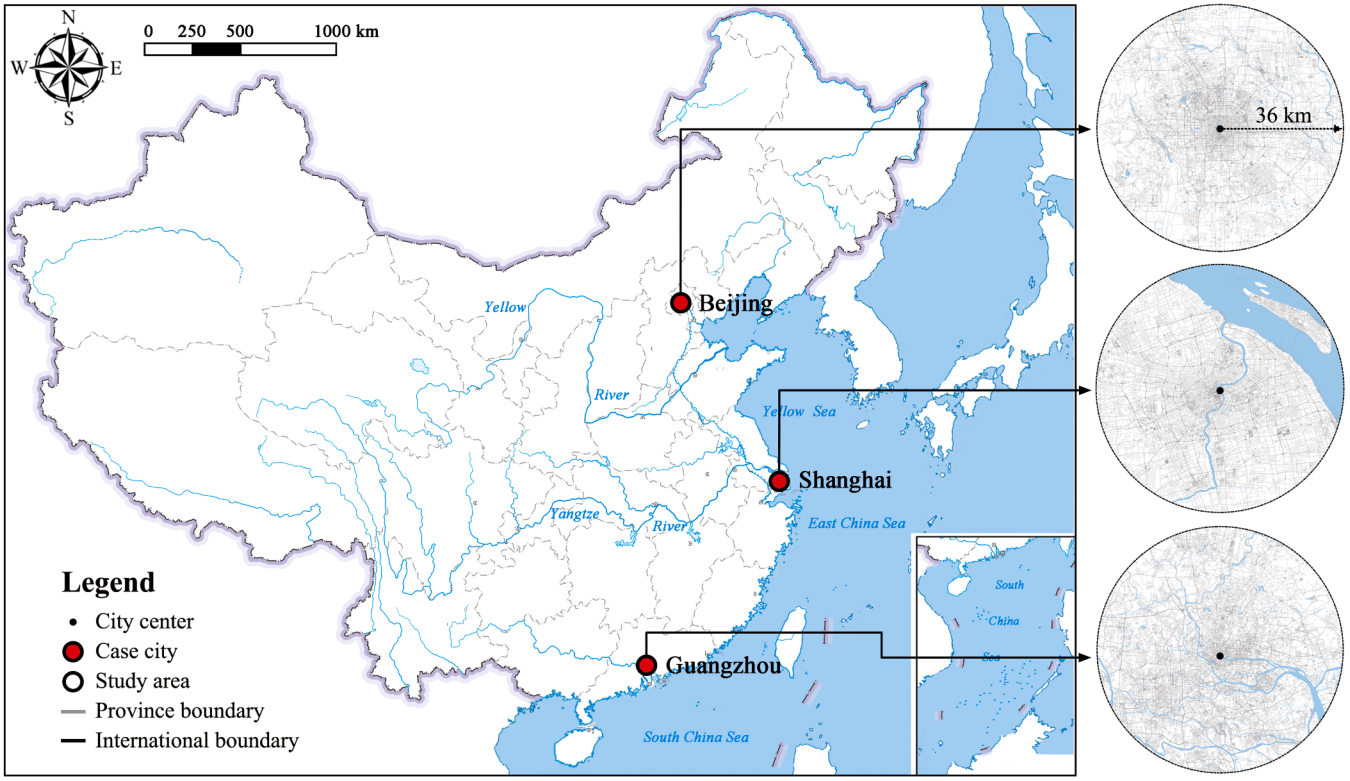


Fig. 1. Location of Beijing, Shanghai and Guangzhou in China, and their respective study area.

Table 1
Data sources and their applications.

Data	Type	Resolution	Source	Period	Application
Keyhole satellite images (7/8)	Grid	0.15–7.5 m	USGS website	1963–1984	Sample labeling
Google historical images	Grid	0.15–1 m	Google Earth	2000 -	Sample labeling
Landsat satellite images (5/7/8)	Grid	15–120 m	USGS website	1984 -	Machine learning
Sentinel satellite images (1/2)	Grid	5–60 m	USGS website	2014 -	Machine learning
POI data	Vector	—	Baidu Map	2018 -	Validation and rectification

multispectral satellite imagery dates back to 1984. Thus, the study period spans from 1985 to 2020. Although higher temporal resolution would offer more precise insights into changes in urban morphology, it would also substantially increase the workload in data processing and analysis. To balance this trade-off between temporal coverage and analytical feasibility, we adopted a five-year interval. To minimize interference from seasonal variations, such as snow and ice, and to avoid cloud cover obscuring surface features, only imagery with less than 10 % cloud cover from May to November in target years (e.g., 1985, 1990, 2015, 2020) was selected. Supplementary datasets, such as vector point-of-interest (POI) data for existing buildings, roads, and other features, were primarily sourced from Baidu Map and extracted using API tools. All data underwent preprocessing, including image mosaicking, georeferencing, and ROI (region of interest) clipping, before analysis.

2.3. Methods

The methodology involves three steps: urban morphology classification, urban redevelopment identification, spatial zonal and statistics (Fig. 2).

2.3.1. The adapted LCZ and classification of urban morphology

We employ an adapted Local Climate Zone (LCZ) scheme to meet the morphological requirements of urban studies. Based on the specific needs of urban morphology research and the characteristics of the study area, certain indicator thresholds and categories were adapted from the standard LCZ scheme (Appendix Table 1), as outlined in Cai et al. (2022). The adapted LCZ' scheme consists of two major categories and ten subcategories. The two primary categories—Built-up and Natural landcover—align with traditional two-dimensional urban morphology studies, highlighting features such as overall land use distribution and spatial structure. The ten subcategories offer a more detailed classification of urban morphology within these broad categories, capturing more specific three-dimensional spatial characteristics of the city. These subcategories include: Compact high-rise (CHR), Compact mid-rise (CMR), Compact low-rise (CLR), Open high-rise (OHR), Open mid-rise (OMR), Open low-rise (OLR), Large low-rise (LLR), Green spaces (GR), Paved and open spaces, Water (Fig. 3).

The urban morphology classification process has three key steps: sample labeling, machine learning, and evaluation feedback (Fig. 2).

1) Sample Labeling. Manually interpreting and labeling samples is the foundation for subsequent machine learning and evaluation. Fig. 3 shows some examples of LCZ' class samples. Because Landsat and Sentinel multi-band remote sensing satellite imagery has a relatively low spatial resolution (5–120 m), it is difficult to manually interpret different LCZ' classes. Therefore, we used super-high-resolution satellite imagery (0.15–7.5 m), like Keyhole and Google historical images, for sample labeling. However, super-high-resolution Google historical images only became available after 2000, and Keyhole

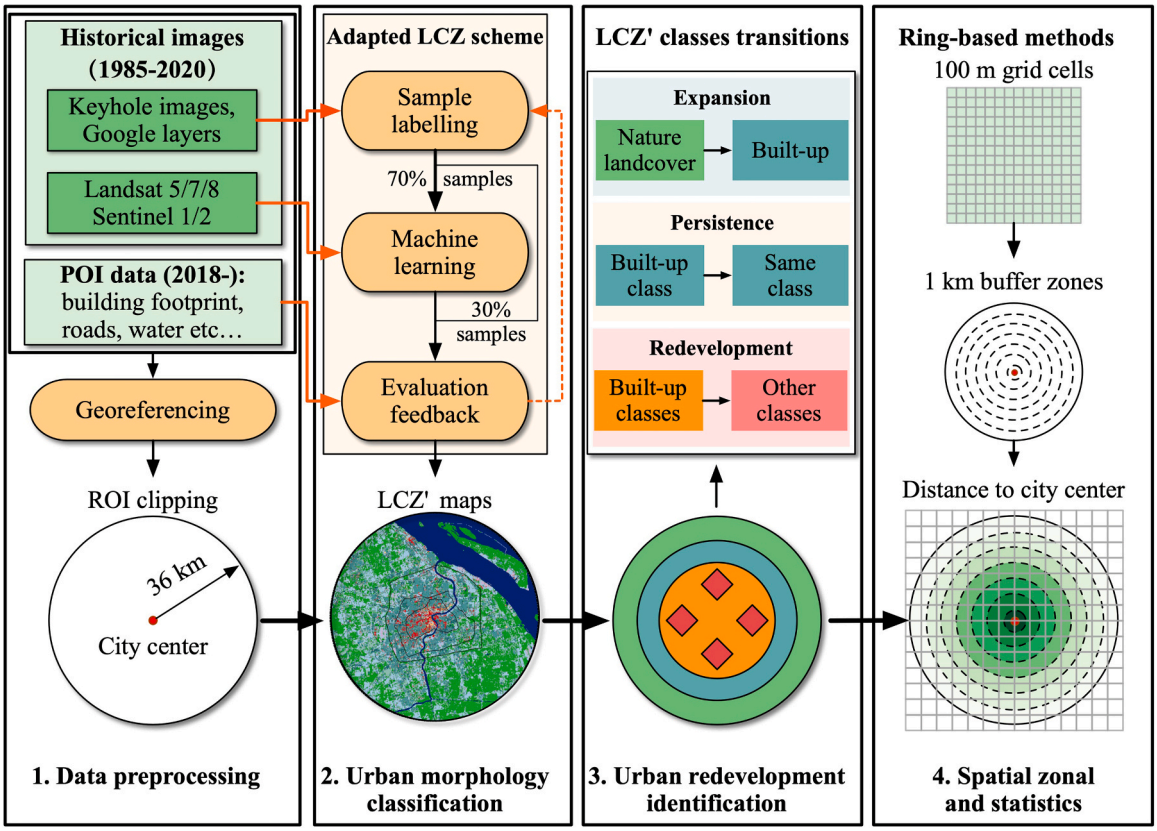


Fig. 2. Workflow of this study and methods.

satellite imagery is limited to 1963–1984. This left a gap in super-high-resolution imagery between 1984 and 2000. To address this, we used an inference method for sample labeling in the 1985–2000 period: we compared super-high-resolution images from before 1984 and 2000 to find areas within the city that had not changed morphologically. We then focused our sample labeling on these stable areas, using them as valid LCZ' samples for 1985–2000. For Beijing, Shanghai, and Guangzhou, we manually labeled 17131, 16364, and 12466 vector samples, respectively.

2) Machine Learning. After manual sample labeling, we used machine learning to handle the large-scale, repetitive task of LCZ' classification. In this stage, we used a random 70 % of the labeled vector samples and multi-band remote sensing satellite imagery (e.g., Landsat 5/7/8 and Sentinel 1/2) as input. The algorithm primarily used for machine learning was an improved version of the LCZ Generator (Demuzere et al., 2021), detailed at https://github.com/matthiasdemuzere/multitemporal-lcz-mapping. The machine learning output consisted of preliminary LCZ maps for the study areas in corresponding years, with a spatial resolution of 100 × 100 m. Due to limitations of machine learning, these initial LCZ' maps often had scattered, disconnected points (sometimes considered noise). To address this, we used spatial filtering to remove these isolated points, making the LCZ' maps better match the real urban morphology and improving classification accuracy.
3) Evaluation Feedback. This step primarily used standard cross-validation methods to assess the accuracy of the machine learning classification. Specifically, the remaining 30 % of the labeled vector samples and the LCZ' maps were used as input to evaluate their consistency. If the accuracy was insufficient, we went back to increase the number of manually labeled samples from the first step and adjusted their spatial distribution, then repeated the machine learning process. To further boost classification accuracy, we integrated recent road and vector building data, and a threshold-based indicator classification method has also been applied to refine the LCZ' categories.

The final classification indicates that the overall accuracy for most LCZ' categories exceeds 65 %, with a weighted overall accuracy of approximately 90 %. For simpler categories, such as green spaces and waterbody, classification accuracy reaches over 85 %, surpassing the 0.5 threshold commonly required in machine learning, and aligning with mainstream remote sensing image recognition standards (Bechtel et al., 2020).

2.3.2. *The identification of urban redevelopment*

During urban development, changes in urban morphology occur not only in the external contours of the city but also through ongoing modifications to the internal LCZ' categories. In this study, we classify the transitions in urban morphology into three categories: expansion, redevelopment, and persistence. "Expansion" refers to the conversion of natural landcover classes, such as green spaces and waterbody, into built-up classes like Compact high-rise (CHR) and Open high-rise (OHR). "Redevelopment" occurs in built-up areas, reflecting changes in the LCZ' categories. For instance, the Open low-rise (OLR) class may be demolished and replaced with Compact mid-rise (CMR) buildings. "Persistence" refers to areas where LCZ' retain their original class without undergoing any changes.

2.3.3. *Ring-based method*

We applied the ring-based method to capture the spatial distribution of LCZ' classes. Specifically, the ring-based method takes the city center as the origin and creates several 1 km-wide buffer zones radiating outward (Fig. 2). This approach is used to statistically analyze the composition and area changes of LCZ' classes within each zone. We quantified and analyzed the volume and location of intra-urban redevelopment to better understand its characteristics. The formulas used are:

LCZ' class	Schematic diagram	Samples	Definitions	LCZ' class	Schematic diagram	Samples	Definitions
B1. Compact High-rise (CHR)			Dense mix of tall buildings to tens of stories. Few or no trees. Land cover mostly paved. Zone function is usually commercial or office.	B4. Open High-rise (OHR)			Open arrangement of tall buildings to tens of stories. Abundance of pervious land cover (low plants, trees). Zone function is usually residential.
B2. Compact Mid-rise (CMR)			Dense mix of mid-rise buildings (3-9 stories). Few or no trees. Land cover mostly paved. Zone function is usually commercial or office.	B5. Open Mid-rise (OMR)			Open arrangement of mid-rise buildings (3-9 Stories). Abundance of pervious land cover (low plants, scattered trees). Zone function is usually residential, education or office.
B3. Compact Low-rise (CLR)			Dense mix of low-rise buildings (1-3 stories). Few or no trees. Land cover mostly paved. Zone function is usually residential.	B6. Open Low-rise (OLR)			Open or sparse arrangement of low-rise buildings (1-3 stories). Abundance of pervious land cover (low plants, scattered trees). Zone function is usually residential.
B7. Large Low-rise (LLR)			Open arrangement of large low-rise buildings or mid-rise industrial structures (1-3 stories). Few or no trees. Land cover mostly paved or hard-packed. Zone function is usually industrial, warehouse or logistics.	N1. Green spaces (GR)			Heavily or lightly wooded landscape of deciduous and/or evergreen trees. Land cover mostly pervious with low plants or grass. Zone function is natural forest, tree cultivation, agriculture or urban park.
N2. Paved and open spaces			Featureless landscape of rock, soil, sand or paved cover. Few or no trees or plants. Zone function is natural desert, demolishing area or urban transportation.	N3. Water			Large, open water bodies such as seas and lakes, or small bodies such as rivers, reservoirs, and lagoons.

Fig. 3. The adapted LCZ' scheme and its corresponding schematic diagram, labeled sample examples and definitions (B1-B7 are built-up classes, N1-N3 denotes natural landcover classes).

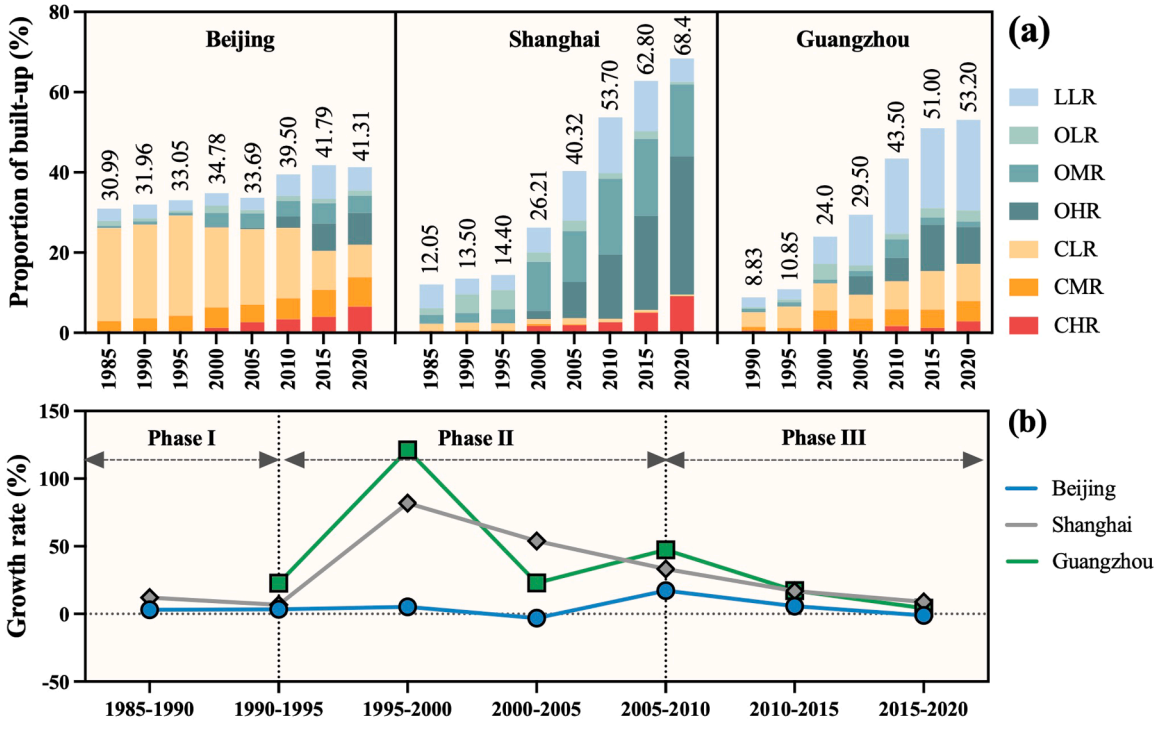


Fig. 4. The proportion of built-up area (a) and its growth rate (b) in Beijing, Shanghai and Guangzhou from 1985 to 2020.

$$V = \sum_{D=1}^{36} N_D \quad (1)$$

$$\overline{D} = \frac{\sum_{D=1}^{36}(D \times N_D)}{V} \quad (2)$$

where V represents the total volume (or number) of redeveloped LCZ' classes within the study area. D indicates the distance to city center, and N_D is the volume (or number) of redeveloped LCZ' classes within each buffer zone. $\overline{D}$ denotes the average distance of redevelopment from the city center.

3. Results

To uncover the characteristics and patterns of urban redevelopment in rapidly developing megacities, we first analyze urban development characteristics by examining the composition and spatial distribution of various LCZ' classes, and then summarize their redevelopment patterns across different cities.

3.1. The development characteristics of Chinese megacities

Over the past 35 years, Chinese megacities have experienced rapidly urbanization, resulting in the transformation of numerous rural green spaces into urban built-up areas and the redevelopment of most older urban centers. Specifically, the proportion of built-up areas in Beijing, Shanghai and Guangzhou has increased from 30.9 %, 12.05 % and 8.83–41.31 %, 68.4 % and 53.2 %, respectively (Fig. 4a). Concurrently, urban redevelopment has significantly changed the dominant LCZ' classes within these built-up areas. Beijing, for instance, transitioned from primarily Compact Low-Rise (CLR) to a mix of Compact Mid-Rise (CMR), Compact High-Rise (CHR), and Open High-Rise (OHR). Shanghai saw a shift from Large Low-Rise (LLR) to OHR. Meanwhile, Guangzhou's dominant LCZ' class evolved from CLR to a combination where CLR and OHR are equally prominent.

Based on the common developmental characteristics associated with urban expansion and redevelopment, the evolution of Chinese megacities can be categorized into three phases: slow redevelopment (Phase I), rapid expansion (Phase II), and decelerated expansion (Phase III) (Fig. 4b). This classification reflects the growth rate of built-up areas, which initially shows a stable trend, followed by an increase, and ultimately a decline. For instance, in Beijing, the five-year growth rate of built-up areas rose from 3.13 % (1985-1990) to 17.22 % (2005-2010), before decreasing to -1.15 % (2015-2020). The negative growth rate is primarily due to Beijing's "reduction-oriented development" and "demolition for green" policies implemented in recent years (The People's Government of Beijing Municipality, 2017), which aims to curb urban sprawl, enhance land-use efficiency, and improve urban ecological quality. This resulted in the demolition of large parts of built-up areas, subsequently converting them into green and open spaces.

Phase I emerged prior to the 1990s, a period characterized by slow urban development due to relatively modest economic growth. During this phase, most of the urban areas under study remained largely unchanged, with only small areas undergoing expansion and redevelopment. Notably, internal redevelopment within existing urban fabrics surpassed external expansion (Fig. 5). For instance, in Beijing, the percentage of redevelopment areas was 15.9 % between 1985 and 1990, and 13.7 % from 1990 to 1995, while the percentage of areas experiencing expansion during these two periods was only 8.9 % and 8.4 %, respectively. This developmental pattern was similarly observed in Shanghai and Guangzhou. Due to the sluggish pace of development, the built-up area increased in Beijing (from 30.9 % to 31.8 %), Shanghai (from 12.1 % to 14.4 %), and Guangzhou (from 8.8 % to 10.8 %). Additionally, the percentages of each LCZ' class exhibited only minor changes; for example, the Compact low-rise (CLR) class experienced increases of merely 1.7 %, 1.68 %, and 0.03 % in Beijing, Shanghai, and Guangzhou, respectively.

After 1995, following the deepening of China's economic reform and the emergence of the land finance system, China gradually entered a period of rapid expansion (Phase II). During this phase, the five-year average growth rates of built-up areas surged to 6.44 %, 56.33 %, 63.87 % in Beijing, Shanghai and Guangzhou (Fig. 4b), respectively. Notably, the percentage of areas undergoing expansion began to exceed that of redevelopment (Fig. 5). For example, in Shanghai, the percentages of expansion and redevelopment in the study area were 5.3 % and 15.2 %, respectively, during the 1990–1995 period. However, by the 2000–2005 period, these figures had shifted to 16.2 % for expansion and 14.1 % for redevelopment. From 1995–2010, this rapid urban expansion led to increases in built-up areas, growing from 33.05 % to 39.50 % in Beijing, from 14.40 % to 53.70 % in Shanghai, and from 10.85 % to 43.50 % in Guangzhou. Simultaneously, inner urban areas experienced significant redevelopment, with numerous regions being demolished and reconstructed. This transformation resulted in substantial changes to the LCZ' composition; for instance, the percentage of the Compact low-rise (CLR) class decreased from 24.9 % to 17.6 % in Beijing and from 1.68 % to 0.75 % in Shanghai.

After 15 years of rapid expansion, the shortage of land supply has become increasingly evident. Coupled with a slowdown in economic growth, the development of Chinese cities has entered a new phase, characterized by a shift to decelerated expansion (Phase III), where urban redevelopment now outweighs expansion. For instance, during the 2015–2020 period, 24.2 % of the area in Guangzhou underwent redevelopment, while only 9.2 % saw expansion (Fig. 5c). Over the past decade of urban redevelopment, several lower construction intensity LCZ' classes (e.g., OLR and CLR) have been replaced by higher construction intensity LCZ' classes (e.g., OHR and CHR). This transition has led to a decrease in the percentage of CLR, which fell from 17.5 % to 8.1 % in Beijing and from 0.75 % to 0.35 % in Shanghai, respectively.

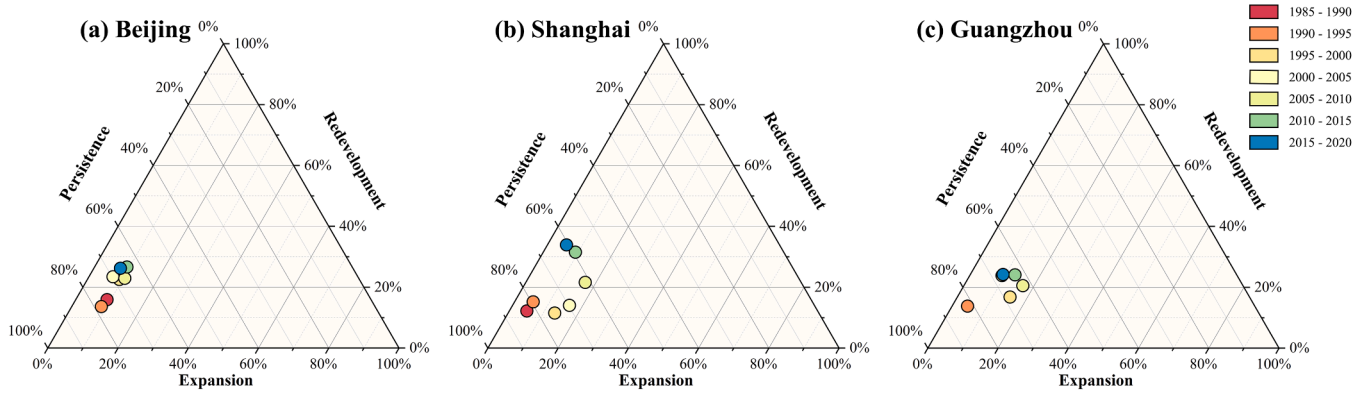


Fig. 5. Ternary scatter plot of urban redevelopment, expansion and persistence area in Beijing (a), Shanghai (b) and Guangzhou (c) from 1985 to 2020.

3.2. The redevelopment characteristics of Chinese megacities

3.2.1. The spatiotemporal distribution of urban redevelopment area

Coupled with urban development and the three phases of evolution, redevelopment areas gradually shifted from central urban areas to suburban areas. In Phase I (1985–1995), the redevelopment areas were relatively homogeneous, both in urban and suburban areas, characterized by a low level of redevelopment and few hotspots (Fig. 6). In Phase II (1995–2010), the expansion of redevelopment areas began to shift outward from the city center to the suburbs. For example, as illustrated in Fig. 6, the hotspots for redevelopment in Beijing were initially located between the 3rd and 4th ring roads, before gradually moving to the area between the 4th and 5th ring roads. After 2010, as Chinese megacities transitioned into Phase III, redevelopment primarily occurred in suburban areas. In Beijing, this included regions between the 5th and 6th ring roads; in Shanghai, areas outside the 3rd ring road; and in Guangzhou, zones situated between the inner and outer ring roads.

3.2.2. The vertical redevelopment characteristics of LCZ' classes

Due to the unique characteristics of each city, the dominant LCZ' classes vary across different cities. However, a common pattern emerges: LCZ' classes with lower construction intensity are gradually replaced by those with higher construction intensity, a trend that can be described as a gradual redevelopment pattern. In the early years, particularly during Phase I, CLR class was predominantly transformed into CMR class to create more usable space by building upward. For instance, between 1990 and 1995, the CLR class accounted for 2.65 % of the study area in Beijing and 4.21 % in Guangzhou. As the percentage of CLR decreased and that of CMR increased, the number of CMR areas being transformed into CHR class also rose, reaching 0.91 % in Beijing and 0.41 % in Guangzhou between 2015 and 2020.

In addition to the gradual redevelopment, other types of urban redevelopment exist, including vertical backward redevelopment and vertical leapfrog redevelopment. Vertical backward redevelopment involves built-up LCZ' classes converting to natural landcover LCZ' classes, often referred to as "demolition for green," typically driven by urban planning and regulatory requirements; for example, CLR and OLR classes transform into green spaces. Figs. 7–9 illustrate numerous areas undergoing backward redevelopment, especially prominent during Phase I and Phase III—where in Beijing and Guangzhou, backward redevelopment mostly occurred in the CLR class, comprising 6.25 % and 0.47 % of the study area during the 1990–1995 period, respectively. In Shanghai, this trend was more evident in the OLR class, accounting for 2.73 % of the study area during the same period. On the other hand, vertical leapfrog redevelopment refers to the transformation of the lowest construction intensity LCZ' classes directly into the highest construction intensity classes; for instance, the CLR transformed into CHR in Beijing and Guangzhou, while the OLR transitioned to OHR in Shanghai. Unlike gradual and backward redevelopment, which appeared across all phases, the vertical of leapfrog redevelopment primarily emerged in Phase III, aiming to increase land development intensity and create more usable space as land resources become increasingly scarce.

3.2.3. The horizontal and spatiotemporal redevelopment direction of LCZ' classes

Similarly to the vertical characteristics of redevelopment in LCZ' transformations, gradual, leapfrog, and backward redevelopment also manifested in the horizontal aspect, particularly in terms of spatiotemporal redevelopment directions.

In Phase I (1985–1995), the redevelopment LCZ' classes were primarily CLR and LLR across all cities, albeit with varying redevelopment directions for different LCZ' classes (Fig. 10). For CLR, central area CLR was mainly replaced by CMR, with a gradual shift from central areas to suburban areas. This redevelopment characteristic was particularly pronounced in Beijing and Guangzhou. Similar to central area, rural and suburban CLR have also experienced gradual redevelopment, while rural CLR was mainly transformed into green spaces, and the suburban CLR shifted towards LLR or OMR (Fig. 10c and Fig. 10l). For LLR, their predominance was observed in suburban and rural areas, where

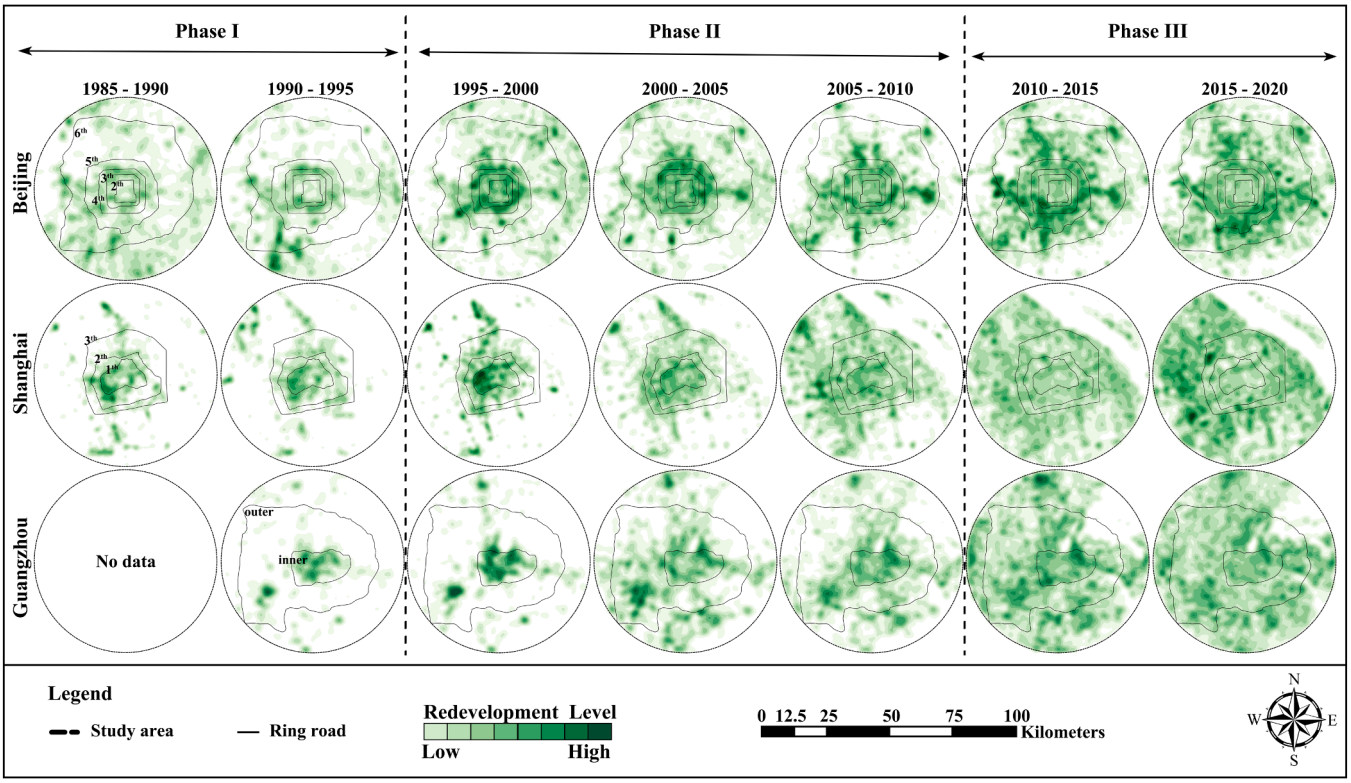


Fig. 6. The hotspots and spatiotemporal distribution of urban redevelopment area in Beijing, Shanghai and Guangzhou.

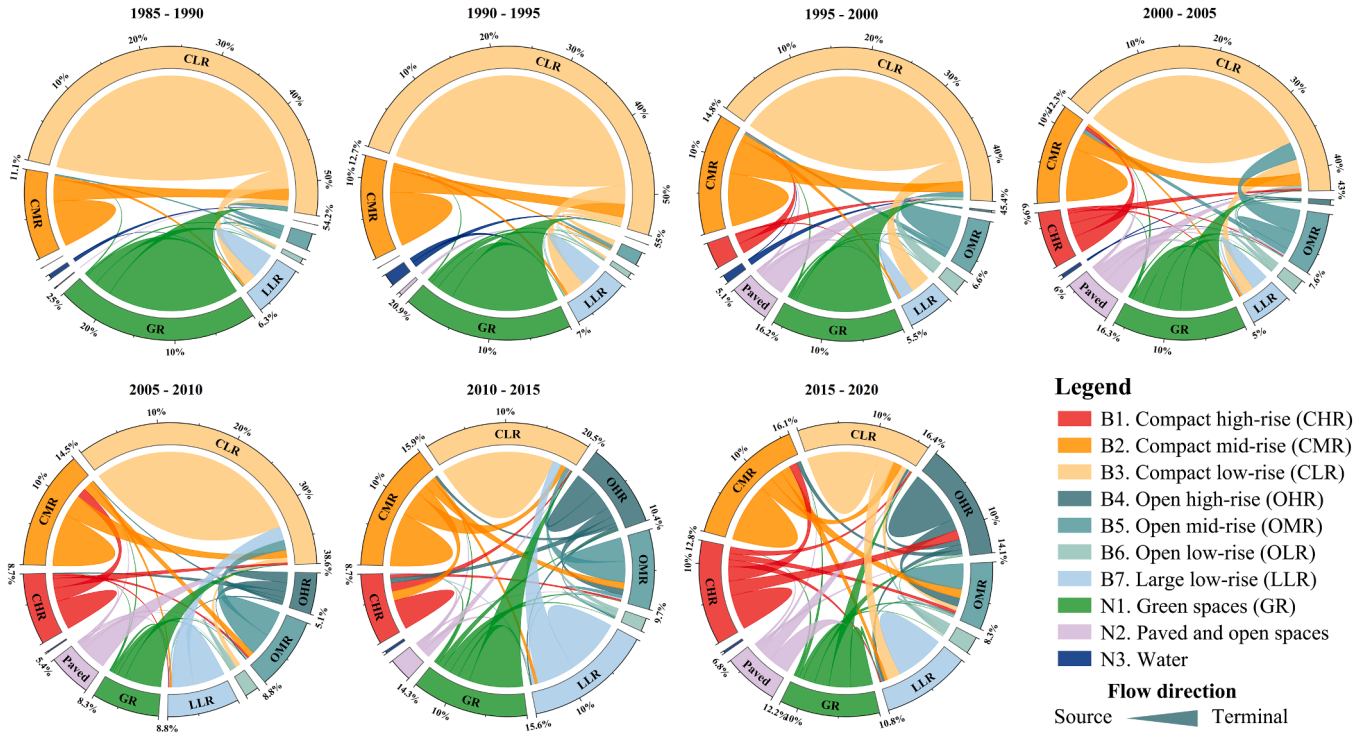


Fig. 7. The redevelopment of LCZ' classes in Beijing from 1985 to 2020.

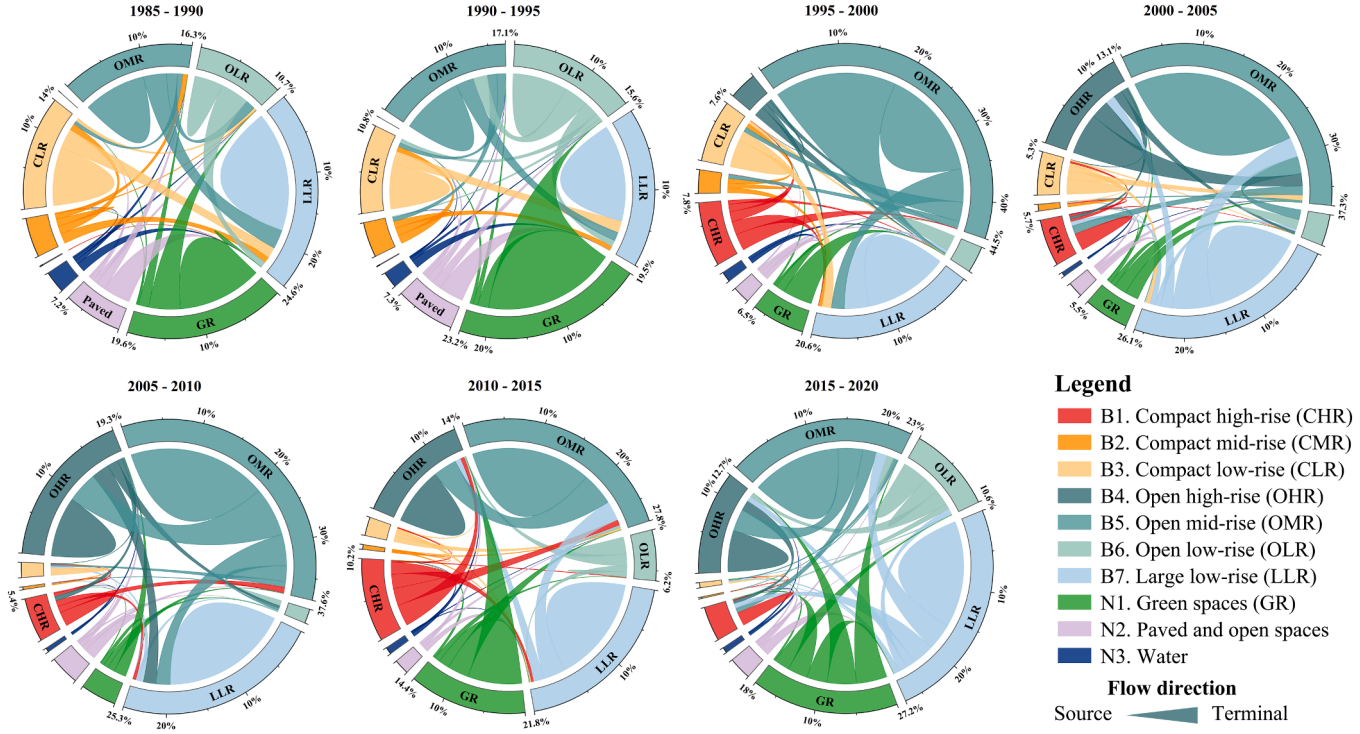


Fig. 8. The redevelopment of LCZ' classes in Shanghai from 1985 to 2020.

suburban LLR was primarily reconstructed into CLR like in Beijing, maintaining a stable area in this early phase and moving from suburban to central areas. Rural LLR, however, was often transformed into green spaces, with a redevelopment direction shifting from inner to outer areas (Fig. 10e, Fig. 10j, and Fig. 10o).

In Phase II (1995–2010), as CLR declined, LLR gradually became the dominant redevelopment LCZ' class. This characteristic more likely appeared in Beijing and Guangzhou, since they have numerous CLR and LLR. Over this period, most suburban LLR underwent backward then gradual redevelopment, progressively moving from rural areas to the central areas, then from inner to outer areas (Fig. 10c, o).

After 2010, Chinese megacities entered Phase III, with a noticeable decrease in CLR class, which became more concentrated in historical zones and rural residential areas. The demolition of CLR housing to

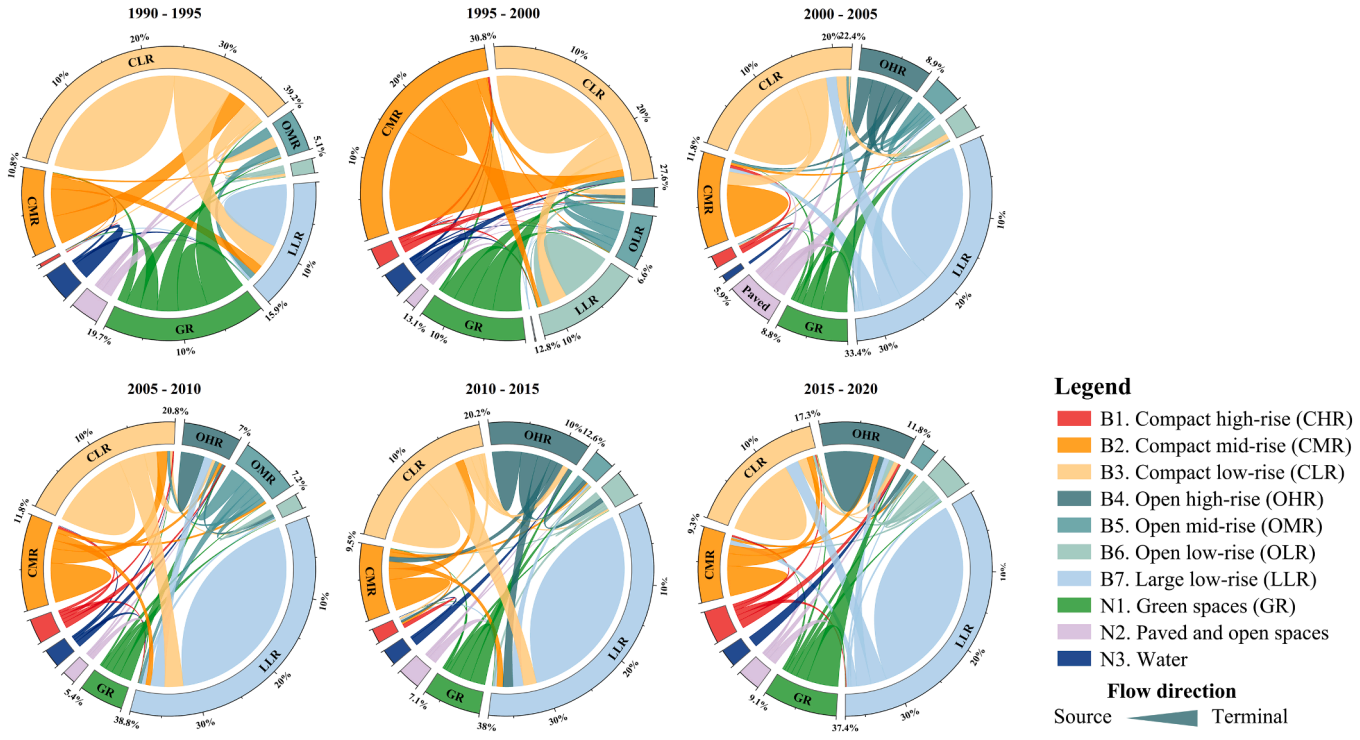


Fig. 9. The redevelopment of LCZ' classes in Guangzhou from 1990 to 2020.

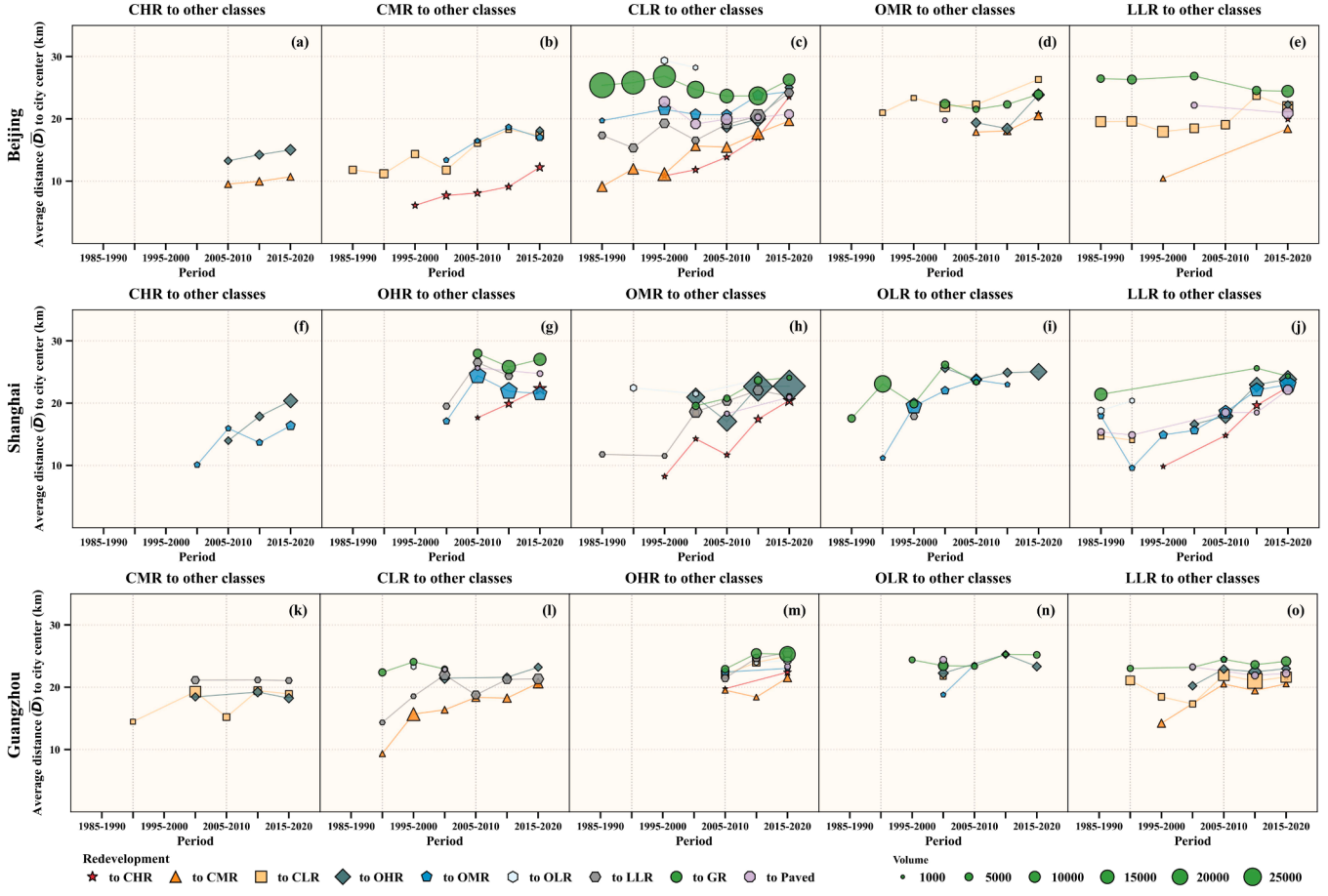


Fig. 10. The spatiotemporal redevelopment of LCZ' classes in Beijing, Shanghai and Guangzhou from 1985 to 2020.

create industrial or logistics zones has become increasingly unsustainable, leading to a great reduction in transformations from CLR to LLR. Additionally, the completion of "demolition for green" initiatives in the suburbs shifted backward CLR redevelopment toward rural areas. In urban central areas, some CMR and CLR directly transformed into CHR classes, as Fig. 10b-c show in Beijing city. With the transformation and upgrading of urban industries, conflicts between industrial and logistics land use within cities and functional positioning of core urban areas became more prominent, resulting in a renewed focus on the redevelopment of these areas and a shift back in redevelopment direction toward LLR within the city, as Fig. 10e-o showed in Beijing and Guangzhou city, respectively.

Comparing redevelopment phases in Beijing, Shanghai, and Guangzhou over the past 35 years reveals regional differences: Beijing emphasizes redevelopment of compact classes, Shanghai focuses on open and LLR redevelopment, while Guangzhou prioritizes both compact and LLR redevelopment. These differences stem from distinct urban development policies and governance approaches—Beijing adopts a stock-based and even reduction-oriented development policy, imposing stringent restrictions on urban population growth and land expansion, prompting compact redevelopment strategies. In contrast, Shanghai's approach reflects low-density, suburbanization development strategies inspired by Western models. Meanwhile, Guangzhou's scenario showcases relatively weak governmental control, leading to market-driven forces and the proliferation of high-density informal constructions and LLR industrial land use. However, it is essential to note that the overall pattern of LCZ' class redevelopment adheres to a "gradual" development logic, highlighting a trend of outward expansion from city centers and progression toward higher-intensity construction zones. This typically involves a shift from low-intensity LCZ' classes (e.g., CLR and LLR) to high-intensity classes (e.g., CMR and CHR). Besides this gradual pattern, unique redevelopment practices—such as "demolition for green" in the suburban CLR and LLR areas of Beijing—start from the suburbs and move towards central areas.

4. Discussions

4.1. The redevelopment trends of Chinese megacities

By comparing the rapidly urbanizing megacities of Beijing, Shanghai, and Guangzhou, we can observe that urban morphology generally follows a redevelopment logic of increasing construction intensity (Fig. 11). Due to differences in dominant LCZ' classes, the specific LCZ' classes renewed during various urban development phases differed. In the early stages of urbanization before 1995 (Phase I), these cities experienced limited external expansion, with gradual redevelopments centered around older areas. The renewed LCZ' classes primarily consisted of Compact low-rise (CLR), Large low-rise (LLR), and Open low-rise (OLR), which transformed into Compact mid-rise (CMR) and green spaces, representing both gradual redevelopment and the "demolition for green space" approach, respectively. After the late 20th century (Phase II), as urbanization in China accelerated, large-scale redevelopment began both internally and externally. While cities generally maintained their prior redevelopment approaches, increasing construction intensity led to the emergence of Compact high-rise (CHR) and Open high-rise (OHR) classes on the urban skyline, with some CMR and Open mid-rise (OMR) areas in older urban areas being directly replaced by these higher-intensity classes. Following 2010 (Phase III), as urbanization rates in Beijing, Shanghai, and Guangzhou reached approximately 70 %, coupled with a slowdown in economic growth, the rate of urban expansion visibly decreased. Furthermore, challenges such as land shortages and environmental issues emerged, compelling cities to transition from inefficient, sprawling land development to compact, high-intensity development. In suburban areas, LLR buildings were replaced by OHR, while CLR buildings within urban centers were replaced with CMR and CHR, with some CMR further transitioning into CHR. After nearly forty years of renewal and development, these changes have significantly transformed urban landscapes, leading to the gradual decrease, and even disappearance of unique urban landscapes. Take the CLR class in Beijing as an example: in the early 1990s, most CLR areas were composed of "hutongs" —primarily single-story buildings with dark bricks and gray tiles. Today, their area has drastically decreased, and they are only found within Beijing's Second Ring Road. In contrast, high-rise buildings have proliferated both within and outside the city, gradually leading to a more homogenized "one-size-fits-all" urban landscape across different cities.

4.2. The redevelopment patterns of Chinese megacities

The evolution of LCZ' classes over the past 35 years in Beijing, Shanghai, and Guangzhou highlight that "gradual high-intensity development" is a fundamental characteristic of rapidly developing megacities (Fig. 12). LCZ' transformation and redevelopment indicate a clear trend toward higher construction intensity, where CLR or LLR buildings are rebuilt into OMR and CMR, which can further evolve into the CHR class. In specific cases, leapfrogging transitions occur, allowing areas to move directly from the lowest-intensity class to the highest-intensity class, as seen with CLR transitioning directly to CHR in city centers (Fig. 10c and Fig. 12d). It is important to note that the transformation of LCZ' classes is not always a one-way flow; occasionally, bidirectional flows are observed, with LCZ' classes transitioning both from lower to higher intensity and from higher to lower intensity. Spatially, these two flow types often occur in different locations, leading to a form of spatial misalignment. For example, CLR residential areas in suburban locations may redevelop into LLR due to the relocation of industrial zones, while CLR in urban core areas, especially in city centers, are more likely to be redeveloped into CMR and CHR (Fig. 10c-l).

A further analysis of the LCZ' redevelopment characteristics in

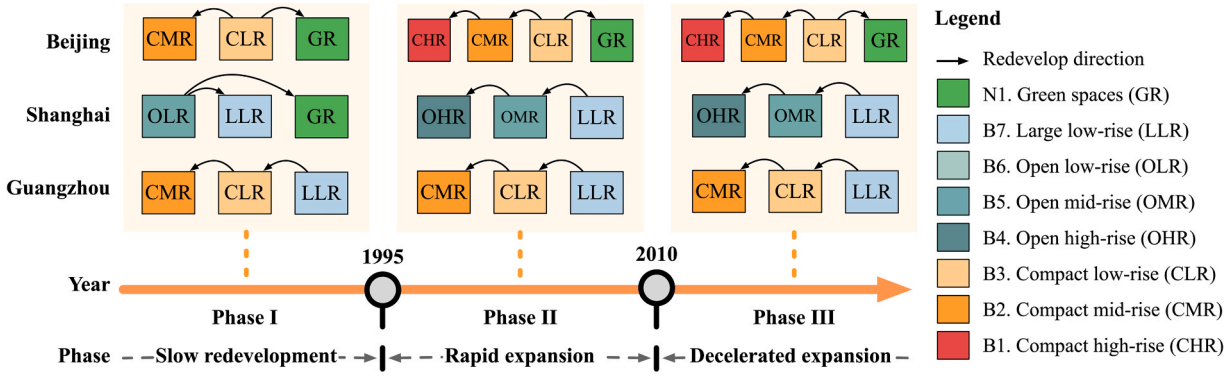


Fig. 11. The redevelopment characteristics in Beijing, Shanghai and Guangzhou across different phase.

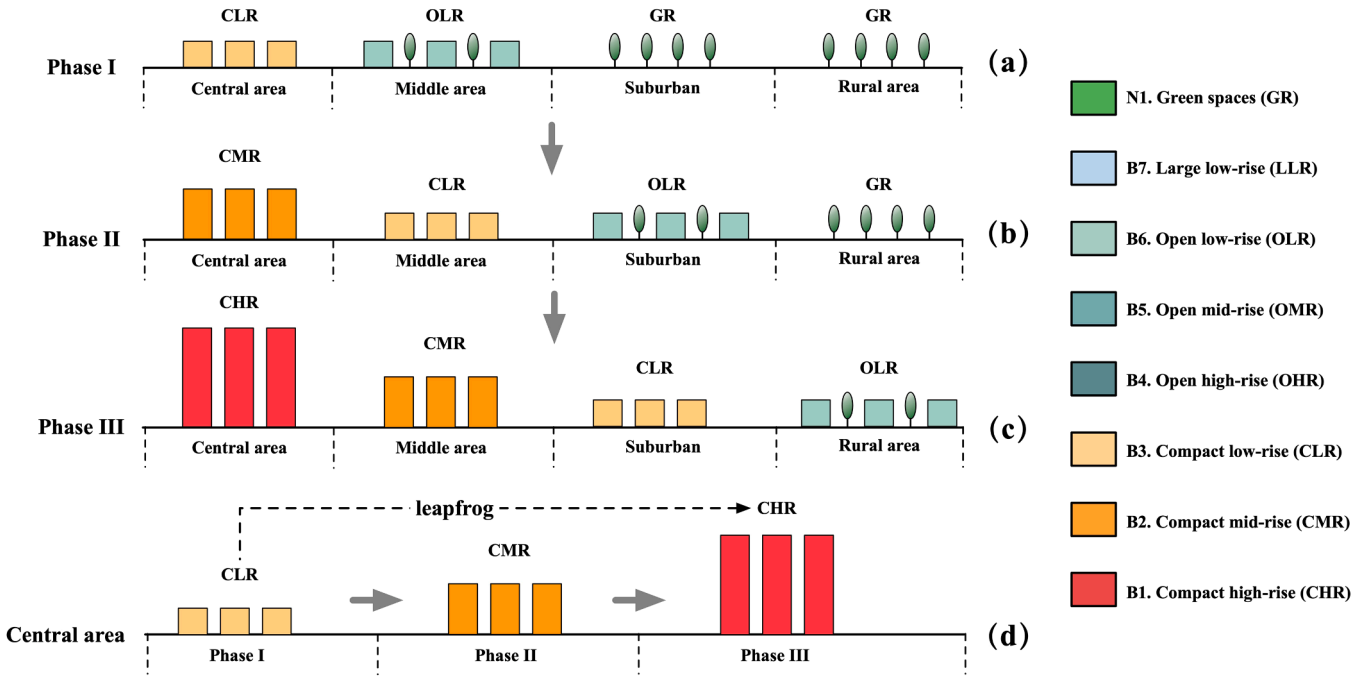


Fig. 12. The "gradual" spatiotemporal distribution of LCZ' (a-c) and leapfrog development of LCZ' in urban central area (d).

Beijing, Shanghai, and Guangzhou across different periods, particularly as illustrated in Fig. 10, reveals three primary patterns in rapidly developing megacities: gradual, "T"-shaped leapfrog, and inverse "T"-shaped leapfrog (Fig. 13).

The gradual pattern typically initiates redevelopment in urban central and surrounding areas, gradually expanding outward toward the suburbs (Fig. 13a), and serves as the dominant approach for the redevelopment of most LCZ' classes. Examples include Beijing's LCZ' transformation from CMR to CHR after 1995 (Fig. 10b), Shanghai's shift from LLR to CHR after 1995 (Fig. 10j), and Guangzhou's transition from CLR to CMR after 1990 (Fig. 10l). Economic factors drive this pattern, as redevelopment in older urban areas can yield significant returns, particularly in high-density urban centers or residential areas, while the likelihood of redevelopment in low-density industrial and rural villa areas remains relatively low (Frantál et al., 2015; Han et al., 2022; Rosenthal and Helsley, 1994).

The "T"-shaped leapfrog pattern begins redevelopment in the central and surrounding areas, moving outward toward the suburbs. At a certain stage, however, a secondary redevelopment occurs around the central area (Fig. 13b). This second wave displaces LCZ' classes that no longer match the city center's functional needs, completing the transformation and functional redevelopment of the core area. This pattern exemplified by Beijing's shift from CLR to CMR since 1985 (Fig. 10c), and Shanghai's OMR to CHR after 1995 (Fig. 10h).

Lastly, the inverse "T"-shaped leapfrog pattern is characterized by simultaneous redevelopments occurring within and outside the city but in opposite directions; inner-city redevelopment moves outward from the center while outer-city redevelopment progresses inward toward the central area (Fig. 13c), resulting in renewed urban and suburban areas causing LCZ' transitions back to outlying suburban zones. Examples include Guangzhou's transition from LLR near the center to CMR, alongside the transformation of LLR in suburban areas back to CLR after 1995 (Fig. 10o).

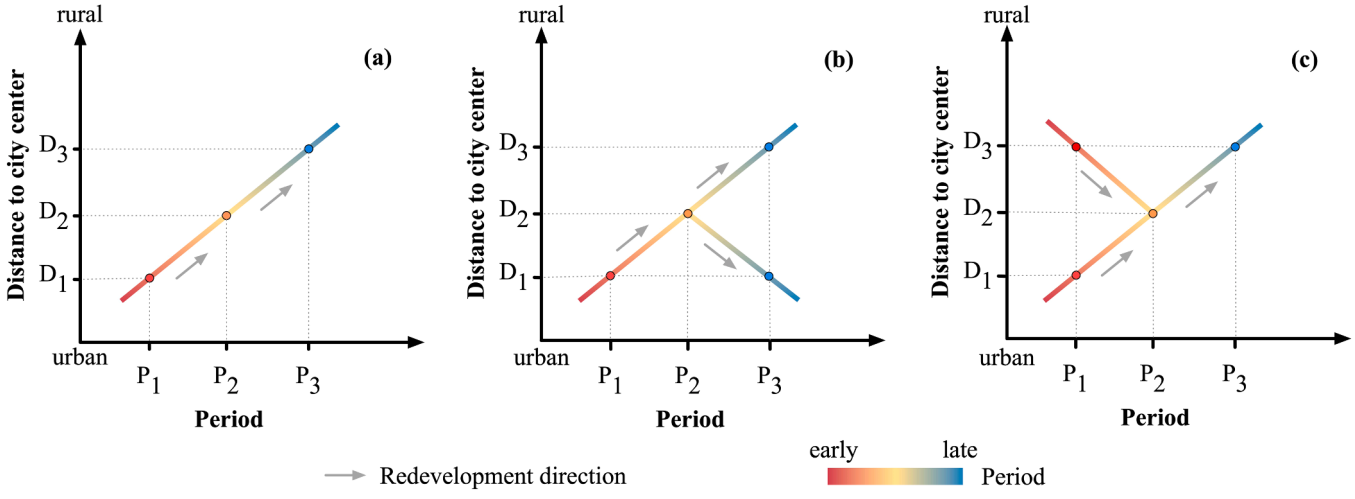


Fig. 13. Three spatiotemporal redevelopment patterns of LCZ': Gradual (a), "T"-shaped leapfrog (b), and inverse "T"-shaped leapfrog (c).

4.3. The driving forces of urban redevelopment patterns

Urban redevelopment is influenced by a multitude of factors, including economic conditions, policies, and property rights. For redevelopment projects, development costs and potential returns are two primary considerations. Typically, city centers possess significant locational advantages. Although land redevelopment costs in these areas are high, the potential for substantial returns after redevelopment is also considerable, leading stakeholders to prioritize initial redevelopment efforts in central urban areas (Frantál et al., 2015). However, following early redevelopment, the costs for subsequent redevelopment in center city areas rise sharply, and the potential for returns is significantly compressed. This drives redevelopment activities to gradually shift from the city center towards its periphery (Rosenthal and Helsley, 1994), manifesting as a gradual redevelopment pattern. As cities continue to develop and the redevelopment of areas surrounding the city center is completed, the cost difference for secondary development between the city center and its periphery gradually diminishes, while the disparity in returns widens. Additionally, certain areas within city centers, due to complexities such as fragmented land ownership and coordination difficulties (Lai et al., 2021b), were often neglected during early redevelopment phases. When secondary redevelopment of these central areas eventually becomes feasible, it exhibits a "T"-shaped leapfrog redevelopment pattern. In contrast, suburban redevelopment displays a distinctly different characteristic: moving from outer to inner areas. This is primarily because suburban areas contain a large number of inefficiently utilized built-up lands, predominantly characterized by OLR and LLR class. These inefficient land in the outer suburbs possess advantages such as better external transportation access and lower population density. Compared to inner suburban areas, they offer greater redevelopment potential and are more likely to develop into new towns in early phases (Han et al., 2022), gradually expanding towards the central urban areas. Furthermore, to secure greater profits, redevelopment activities in inner suburban areas are more prone to resistance from local residents (Wang et al., 2022), which delays the redevelopment process, thereby exhibiting an inverse "T"-shaped leapfrog redevelopment pattern.

4.4. Policy implications

In practical terms, our findings offer actionable insights for urban planners and policymakers. First, when optimizing urban morphology, it is essential to conduct systematic evaluations (e.g., landscape characteristics and economic cost), and then propose targeted strategies based on LCZ' classes and their redevelopment patterns. Taking CLR and LLR in central urban areas as examples: CLR class is typically located within historical areas, necessitating preservation efforts instead of redevelopment. In contrast, the LLR class often differs significantly in landscape character from the surrounding central areas and are functionally mismatched with them, suggesting that redevelopment could be the primary optimization approach. Second, the morphology-based LCZ' scheme can bridge the gap between two-dimensional and three-dimensional urban morphology control. For example, LCZ' can be utilized to establish a corresponding planning and control system, providing flexible supplements to existing master plans, regulatory plans, and urban design guidelines, along with supporting regulations. At the master plan level, it can guide the sequencing of land development/redevelopment in accordance with urban development patterns, ensuring a rational distribution of various LCZ' classes. At the regulatory plan level, each LCZ' class can serve as a fundamental unit for urban landscape management. By superimposing socioeconomic attributes like property rights and building age, differentiated management strategies can be formulated for each unit (Tian, 2021). At the urban design level, the LCZ' indicator system can be expanded to include metrics like sky view factor and street canyon height-to-width ratios to control sightlines and interfaces. Furthermore, the classification of LCZ' can be refined to incorporate considerations such as building layout and color, thereby enabling precise shaping and control of streetscape characteristics. Finally, our study also offers ecological implications: urban development should balance high-intensity redevelopment with ecological initiatives like "demolition for green" to reduce carbon emissions and mitigate urban heat island effects (Zhang et al., 2025). Overall, our research advances sustainable urban governance in the context of rapid urbanization.

4.5. Limitations and future studies

We utilized satellite remote sensing imagery data and machine learning methods alongside an adapted Local Climate Zone (LCZ) scheme to systematically analyze the characteristics and patterns of urban redevelopment in rapidly developing areas represented by Beijing, Shanghai, and Guangzhou, China. However, there are several limitations to this research. First, regarding data sources, although various image datasets were employed to tackle the challenges of limited data availability for long-term, high spatiotemporal resolution urban studies. However, some imagery data were not fully utilized. For instance, Google super-high-resolution imagery served primarily as a labeling layer, while morphology classification relied mainly on Landsat series images. This limitation contributed to the relatively low accuracy of morphology classification in the machine learning model, which in turn restricted the study period to 1985–2020. Future research should consider employing image fusion techniques to create integrated, super-high-spatiotemporal resolution imagery products to enhance classification accuracy and extend the study period back to 1960. Second, concerning research methodology, to address urban morphology's complexity, this study introduced an adapted LCZ scheme to summarize and decompose urban morphology, classifying it into 10 secondary categories. While this classification is relatively detailed, it does not fully capture certain spatial characteristics of the city; for instance, super-high-rise buildings above 100 m were classified either as compact high-rise or open high-rise in this study. Future research could refine the classification of morphology classes in urban built-up areas for greater precision. Lastly, while this paper focuses primarily on the spatiotemporal distribution characteristics and patterns of urban redevelopment, it does not provide an in-depth analysis of the underlying driving forces. Future studies should explore driving factors from various perspectives, including policy, economics, and stakeholder influences (Li et al., 2014; Van Duijn et al., 2016).

5. Conclusions

In this study, we applied an adapted Local Climate Zone (LCZ) scheme to decode complex urban morphology. By taking three rapidly developing megacities in China—Beijing, Shanghai, and Guangzhou—as case studies, we analyzed the spatiotemporal characteristics and patterns of urban redevelopment, offering new perspectives for understanding urban development and its dynamics. It is evident that cities typically progress through three phases: a pre-urbanization period characterized by slow redevelopment, an urbanization period marked by rapid expansion, and a latter half of urbanization phase where expansion slows. The proportion of urban redevelopment during these phases shows a U-shaped trend, being dominant in Phase I, surpassed by expansion in Phase II, and becoming dominant again in Phase III. Most cities and LCZ' classes adhere to a gradual redevelopment pattern,

where classes with lower construction intensity are progressively replaced by those with higher construction intensity in the vertical aspect. Additionally, the spatial distribution of urban redevelopment tends to expand outward from the city center in the horizontal aspect. Beyond the gradual redevelopment pattern, other patterns are also present in urban areas. For instance, the leapfrog redevelopment pattern entails transforming urban spaces directly from LCZ' classes with the lowest construction intensity to those with the highest construction intensity. Another notable characteristic is the inverse "T"-shaped leapfrog redevelopment trend, where development simultaneously progresses from the suburbs to the city center and vice versa. Furthermore, in the latter half of urbanization phase, there is increasing attention to ecological environments and quality of life, leading to a steady rise in areas designated for "demolition for green".

Our findings provide an empirical reference for protecting distinctive urban landscapes, optimizing urban morphology, and adjusting land use layouts. The redevelopment characteristics and patterns of Chinese cities can also provide empirical lessons/evidence for other cities, especially the cities under rapid urbanization. In guiding future urban redevelopment and renewal, the LCZ' scheme can facilitate shape urban landscapes and visual features systematically, introduce economic cost assessments, and delineate different renewal units, leading to targeted improvement strategies for different urban morphologies. This approach can promote the effective implementation of urban redevelopment projects and foster sustainable urban development.

CRediT authorship contribution statement

He Zhu: Writing – review & editing, Validation, Supervision. **Yan Tang:** Writing – review & editing, Validation, Supervision, Project administration, Funding acquisition. **Zhi Cai:** Writing – original draft, Visualization, Methodology, Investigation, Formal analysis, Data curation, Conceptualization.

Declaration of Generative AI and AI-assisted technologies in the writing process

During the preparation of this work the authors used Gemini 2.5 pro and DeepSeek service in order to improve the language and readability. After using this tool/service, the authors reviewed and edited the content as needed and takes full responsibility for the content of the publication.

Declaration of Competing Interest

The authors declare that they have no known competing financial interests or personal relationships that could have appeared to influence the work reported in this paper.

Acknowledgments

This work was supported by the National Natural Science Foundation of China (Grant No. 52478038, 52578078), National Key Research and Development Program of China (Grant No. 2022YFC3800301, 2024YFC3807900), Major Project of the National Social Science Fund of China (24&ZD148).

Appendix

Table 1
Values of different urban canopy parameters for LCZ' classes (adapted from Stewart et al., 2012)

Adapted LCZ'	Original LCZ	Sky view factor	Aspect ratio	Building surface fraction	Impervious surface fraction	Pervious surface fraction	Height of roughness elements (m)	Terrain roughness class	Surface albedo
B1. CHR	LCZ 1 compact high-rise (CHR)	0.2–0.4	>2	0.4–0.6	o.4–0.6	<0.1	>25	8	0.10–0.20
B2. CMR	LCZ 2 compact mid-rise (CMR)	0.3–0.6	0.75–2	0.4–0.7	0.3–0.5	<0.2	10–25	6–7	0.10–0.20
B3. CLR	LCZ 3 compact low-rise (CLR)	0.2–0.6	0.75–1.5	0.4–0.7	0.2–0.5	<0.3	3–10	6	0.10–0.20
B4. OHR	LCZ 4 open high-rise (OHR)	0.5–0.7	0.75–1.25	0.2–0.4	0.3–0.4	0.3–0.4	>25	7–8	0.12–0.25
B5. OMR	LCZ 5 open mid-rise (OMR)	0.5–0.8	0.3–0.75	0.2–0.4	0.3–0.5	0.2–0.4	10–25	5–6	0.12–0.25
B6. OLR	LCZ 6 open low-rise (OLR)	0.6–0.9	0.3–0.75	0.2–0.4	0.2–0. 5	0.3–0.6	3–10	5–6	0.12–0.25
None	LCZ 7 lightweight low-rise	0.2–0.5	1–2	0.6–0.9	0.2	<0.3	2–4	4–5	0.15–0.35
B7. LLR	LCZ 8 large low-rise (LLR)	>0.7	0.1–0.3	0.1–0.2	0.4–0.5	<0.2	3–10	5	0.15–0.25

(*continued on next page*)

Table 1 (*continued*)

Adapted LCZ'	Original LCZ	Sky view factor	Aspect ratio	Building surface fraction	Impervious surface fraction	Pervious surface fraction	Height of roughness elements (m)	Terrain roughness class	Surface albedo
B6. OLR	LCZ 9 sparsely built (SB)	>0.8	0.1–0.25	0.2–0.3	<0.2	0.6–0.8	3–10	5–6	0.12–0.25
B7. LLR	LCZ 10 heavy industry (HI)	0.6–0.9	0.2–0.5	<0.1	0.2–0.4	0.4–0.5	5–15	5–6	0.12–0.20
N1. Green space (GS)	LCZ A dense trees	<0.4	>1	<0.1	<0.1	>0.9	3–30	8	0.10–0.20
N1. Green spaces (GS)	LCZ B scattered trees	0.5–0.8	0.25–0.75	<0.1	<0.1	>0.9	3–15	5–6	0.15–0.25
N1. Green spaces (GS)	LCZ C bush, scrub	0.7–0.9	0.25–1.0	<0.1	<0.1	>0.9	<2	4–5	0.15–0.25
N1. Green space (GS)	LCZ D low plants	>0.9	<0.1	<0.1	<0.1	>0.9	<1	3–4	0.15–0.30
N2. Paved or open space	LCZ E bare rock or paved	>0.9	<0.1	<0.1	>0.9	<0.1	<0.25	1–2	0.20–0.35
N2. Paved or open space (OS)	LCZ F bare soil or sand	>0.9	<0.1	<0.1	<0.1	>0.9	<0.25	1–2	0.20–0.35
N3. Water	LCZ G water	>0.9	<0.1	<0.1	<0.1	>0.9	-	1	0.02–0.10

Notes: B1-B7 are built-up classes, N1-N3 denotes natural landcover classes.

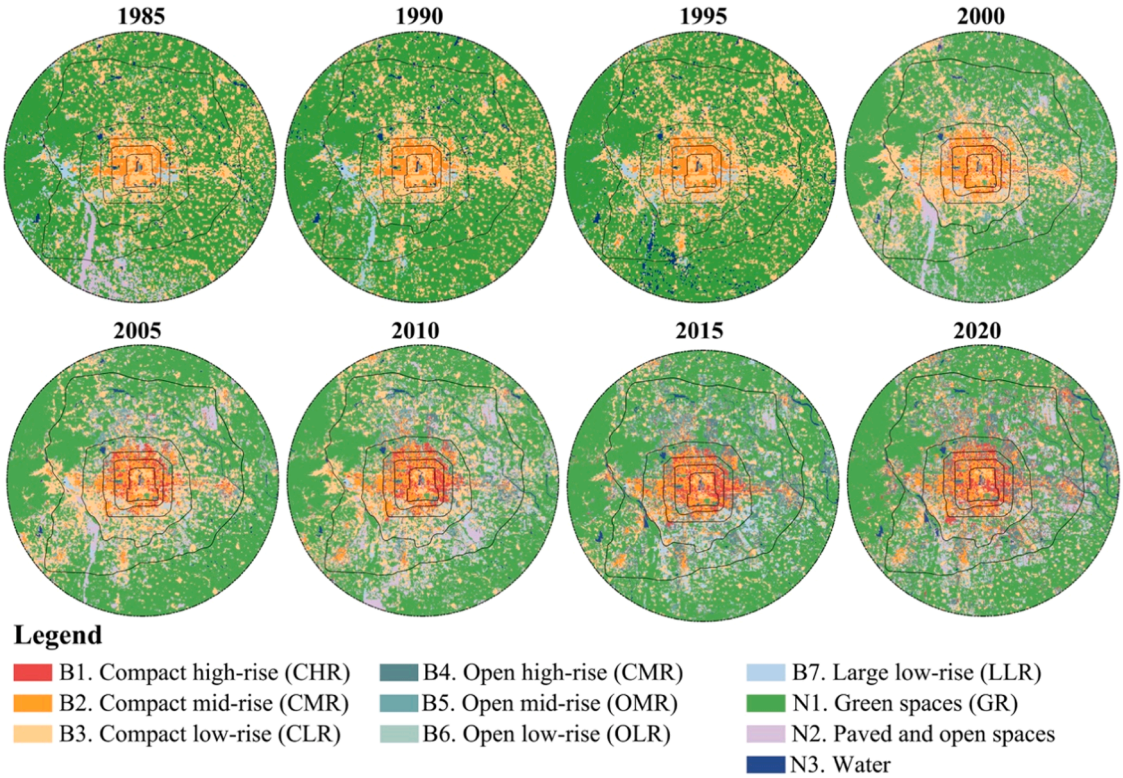


Fig. 1. LCZ' maps for Beijing from 1985 to 2020.

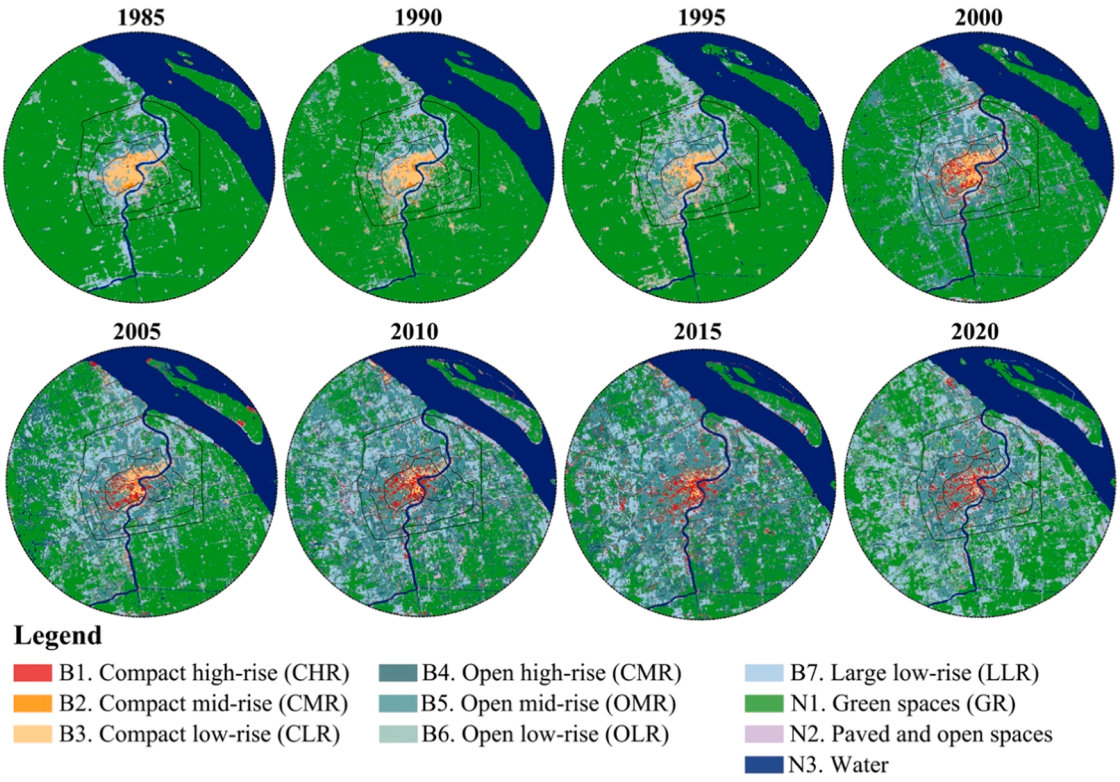


Fig. 2. LCZ' maps for Shanghai from 1985 to 2020.

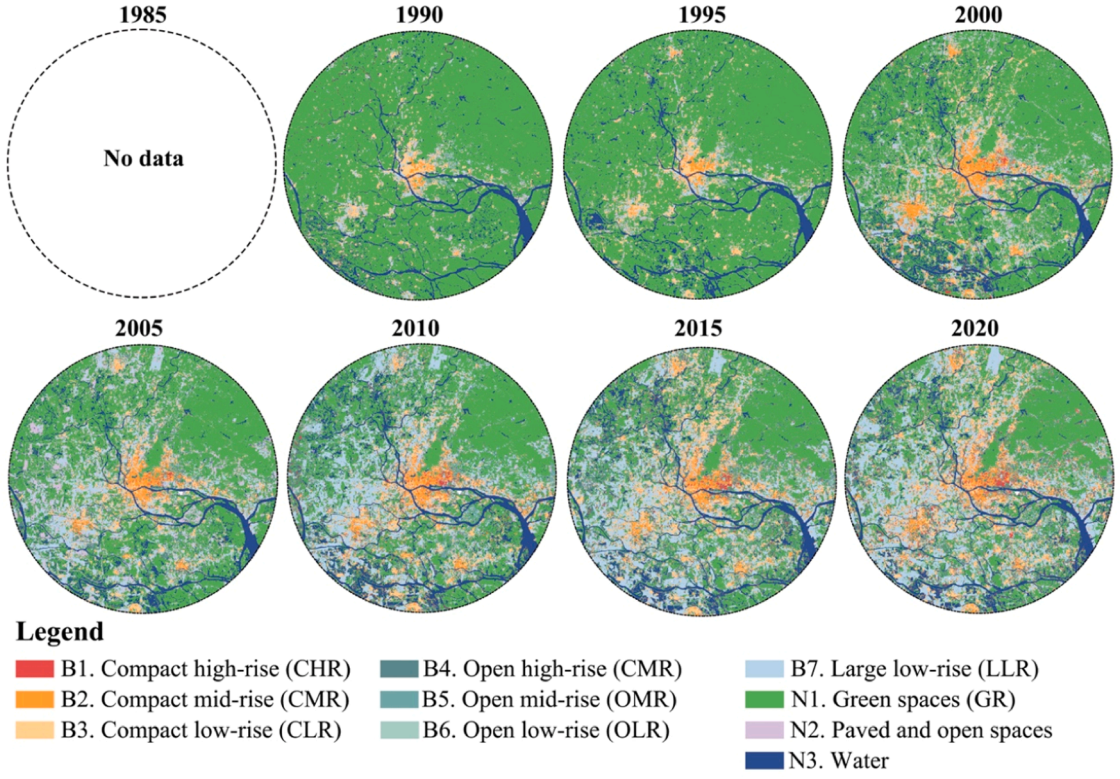


Fig. 3. LCZ' maps for Guangzhou from 1985 to 2020.

Data availability

Data will be made available on request.

References

Alam, T., Banerjee, A., 2023. Characterizing land transformation and densification using urban sprawl metrics in the south bengal region of India. Sustain. Cities Soc. 89, 104295. https://doi.org/10.1016/j.scs.2022.104295.

Bechtel, B., Demuzere, M., Stewart, I.D., 2020. A weighted accuracy measure for land cover mapping: comment on johnson et al. Local climate zone (LCZ) map accuracy assessments should account for land cover physical characteristics that affect the local thermal environment. Remote Sens. 11 (2420), 1769.

Cai, Z., Demuzere, M., Tang, Y., Wan, Y., 2022. The characteristic and transformation of 3D urban morphology in three Chinese mega-cities. Cities 131, 103988. https://doi.org/10.1016/j.cities.2022.103988.

Chen, T.-H.K., Qiu, C., Schmitt, M., Zhu, X.X., Sabel, C.E., Prishchepov, A.V., 2020. Mapping horizontal and vertical urban densification in Denmark with landsat time-series from 1985 to 2018: a semantic segmentation solution. Remote Sens. Environ. 251, 112096. https://doi.org/10.1016/j.rse.2020.112096.

Chen, Y., Zhang, X., Chau, K.W., Yang, L., 2022. How the institutional change in urban redevelopment affects the duration of land redevelopment approval in China? Land Use Policy 119, 106160. https://doi.org/10.1016/j.landusepol.2022.106160.

Demuzere, M., Kittner, J., Bechtel, B., 2021. LCZ Generator: a web application to create Local Climate Zone maps. Front. Environ. Sci. 9, 637455. https://doi.org/10.3389/fenvs.2021.637455.

Dubé, J., Desaulniers, S., Bédard, L.-P., Binette, A., Leblanc, E., 2018. Urban residential reconversion through demolition: a land use model based on administrative spatial micro-data. Land Use Policy 76, 686–696. https://doi.org/10.1016/j.landusepol.2018.02.052.

Frantál, B., Greer-Wootten, B., Klusáček, P., Krejčí, T., Kunc, J., Martinát, S., 2015. Exploring spatial patterns of urban brownfields regeneration: the case of brno, Czech Republic. Cities 44, 9–18. https://doi.org/10.1016/j.cities.2014.12.007.

Han, B., Jin, X., Wang, J., Yin, Y., Liu, C., Sun, R., Zhou, Y., 2022. Identifying inefficient urban land redevelopment potential for evidence-based decision making in China. Habitat Int. 128, 102661. https://doi.org/10.1016/j.habitatint.2022.102661.

Han, Z., Long, Y., Wang, X., Hou, J., 2020. Urban redevelopment at the block level: methodology and its application to all Chinese cities. Environ. Plan. B Urban Anal. City Sci. 47, 1725–1744. https://doi.org/10.1177/2399808319843928.

He, Q., Zeng, C., Xie, P., Tan, S., Wu, J., 2019. Comparison of urban growth patterns and changes between three urban agglomerations in China and three metropolises in the USA from 1995 to 2015. Sustain. Cities Soc. 50, 101649. https://doi.org/10.1016/j.scs.2019.101649.

Heris, M.P., Middel, A., Muller, B., 2020. Impacts of form and design policies on urban microclimate: assessment of zoning and design guideline choices in urban redevelopment projects. Landsc. Urban Plan 202, 103870. https://doi.org/10.1016/j.landurbplan.2020.103870.

Hong, J.-W., Hong, J., 2016. Changes in the Seoul metropolitan area urban heat environment with residential redevelopment. J. Appl. Meteorol. Clim. 55, 1091–1106. https://doi.org/10.1175/JAMC-D-15-0321.1.

Ilic, L., Sawada, M., Zarzelli, A., 2019. Deep mapping gentrification in a large Canadian city using deep learning and google street view. PlOS One 14, e0212814.

Jiao, L., 2015. Urban land density function: A new method to characterize urban expansion. Landsc. Urban Plan 139, 26–39. https://doi.org/10.1016/j.landurbplan.2015.02.017.

Kabisch, N., Haase, D., 2013. Green spaces of european cities revisited for 1990–2006. Landsc. Urban Plan 110, 113–122. https://doi.org/10.1016/j.landurbplan.2012.10.017.

Lai, Y., Tang, B., Chen, X., Zheng, X., 2021b. Spatial determinants of land redevelopment in the urban renewal processes in shenzhen, China. Land Use Policy 103, 105330. https://doi.org/10.1016/j.landusepol.2021.105330.

Lai, Y., Jiang, L., Xu, X., 2021a. Exploring spatio-temporal patterns of urban village redevelopment: the case of shenzhen, China. Land 10, 976. https://doi.org/10.3390/land10090976.

Li, L.H., Lin, J., Li, X., Wu, F., 2014. Redevelopment of urban village in China – a step towards an effective urban policy? A case study of liede village in guangzhou. Habitat Int. 43, 299–308. https://doi.org/10.1016/j.habitatint.2014.03.009.

Lin, L., Di, L., Zhang, C., Guo, L., Zhao, H., Islam, D., Li, H., Liu, Z., Middleton, G., 2024. Modeling urban redevelopment: a novel approach using time-series remote sensing data and machine learning. Geogr. Sustain 5, 211–219. https://doi.org/10.1016/j.geosus.2024.02.001.

Liu, Y., Lin, Y., Fu, N., Geertman, S., Van Oort, F., 2018. Towards inclusive and sustainable transformation in shenzhen: urban redevelopment, displacement patterns of migrants and policy implications. J. Clean. Prod. 173, 24–38. https://doi.org/10.1016/j.jclepro.2016.09.224.

Mele, C., 2013. Neoliberalism, race and the redefining of urban redevelopment. Int. J. Urban Reg. Res. 37, 598–617. https://doi.org/10.1111/j.1468-2427.2012.01144.x.

O'Connor, D., 2019. Phytoremediation: climate change resilience and sustainability assessment at a coastal brownfield redevelopment. Environ. Int. 130.

Rosenthal, S.S., Helsley, R.W., 1994. Redevelopment and the urban land price gradient. J. Urban Econ. 35, 182–200. https://doi.org/10.1006/juec.1994.1012.

Ryan, B.D., 2006. Morphological change through residential redevelopment: detroit, 1951-2000. Urban Morphol. 10, 5–22. https://doi.org/10.51347/jum.v10i1.3924.

State Council, O.L.G.S.C.S.N.P.C., 2021. Major Bechtelures on 2020 Population Census of China. China Statistics Press, Beijing.

Stewart, I.D., Oke, T.R., 2012. Local climate zones for urban temperature studies. Bull. Am. Meteorol. Soc. 93, 1879–1900. https://doi.org/10.1175/BAMS-D-11-00019.1.

The People's Government of Beijing Municipality, 2017. Beijing Urban Master Plan (2016-2035) [WWW Document]. URL,(Accessed 7.31.25). ⟨https://www.beijing.gov.cn/gongkai/guihua/wngh/cqgh/201907/t20190701_100008.html⟩.

Tian, Y., 2021. Management units of urban morphology: significance, formation and application. City Plan. Rev. 45, 9–16.

Van Duijn, M., Rouwendal, J., Boersema, R., 2016. Redevelopment of industrial heritage: insights into external effects on house prices. Reg. Sci. Urban Econ. 57, 91–107. https://doi.org/10.1016/j.regsciurbeco.2016.02.001.

Walker, C.M., Colton Flynn, K., Ovando-Montejo, G.A., Ellis, E.A., Frazier, A.E., 2017. Does demolition improve biodiversity? Linking urban Green space and socioeconomic characteristics to avian richness in a shrinking city. Urban Ecosyst. 20, 1191–1202. https://doi.org/10.1007/s11252-017-0671-4.

Wang, M., Zhang, F., Wu, F., 2022. Governing urban redevelopment: a case study of yongqingfang in guangzhou, China. Cities 120, 103420. https://doi.org/10.1016/j.cities.2021.103420.

Weber, R., 2002. Extracting value from the city: Neoliberalism and urban redevelopment. Antipode. 34 (3), 519–540. https://doi.org/10.1111/1467-8330.00253.

Wen, D., Huang, X., Zhang, A., Ke, X., 2019. Monitoring 3D building change and urban redevelopment patterns in inner city areas of Chinese megacities using multi-view satellite imagery. Remote Sens. 11, 763. https://doi.org/10.3390/rs11070763.

Wong, S.W., Dai, Y., Tang, B., Liu, J., 2021. A new model of village urbanization? Coordinative governance of state-village relations in guangzhou city, China. Land Use Policy 109, 105500. https://doi.org/10.1016/j.landusepol.2021.105500.

Zhang, L., Cai, Z., Huang, H., Lu, Z., Zhai, W., Qin, H., Liu, Z., Tang, Y., 2025. Exploring the characteristics of "demolition for Green" and its impact on urban thermal environments: an empirical study of Beijing, China. Sustain. Cities Soc. 130, 106576. https://doi.org/10.1016/j.scs.2025.106576.

Zhou, C., Zhang, S., Liu, B., Li, T., Shi, J., Zhan, H., 2024. Using deep learning to unravel the structural evolution of block-scale Green spaces in urban renewal. Cities 150, 105030. https://doi.org/10.1016/j.cities.2024.105030.

Zhu, H., Gao, X., Tian, W., Wei, M., Zhang, X., Chen, Y., 2024. Investigating the mechanisms of sustainable urban land renewal: a perspective of spatial development rights. Sustain. Cities Soc. 109, 105536. https://doi.org/10.1016/j.scs.2024.105536.